



ELSEVIER

Available online at www.sciencedirect.com

SCIENCE @ DIRECT®

Physica D 186 (2003) 205–220

PHYSICA D

www.elsevier.com/locate/physd

Dynamical regimes underlying epileptiform events: role of instabilities and bifurcations in brain activity

Jose L. Perez Velazquez^{a,*}, Miguel A. Cortez^a,
O. Carter Snead III^a, Richard Wennberg^b

^a Brain and Behaviour Programme, Division of Neurology, Department of Paediatrics, Hospital for Sick Children, University of Toronto, 555 University Avenue, Toronto, Ont., Canada M5G 1X8

^b Division of Neurology, Department of Medicine, Toronto Western Hospital, 399 Bathurst Street, Toronto, Ont., Canada M5T 2S8

Received 29 July 2002; received in revised form 18 October 2002; accepted 12 February 2003

Communicated by J.P. Keener

Abstract

Epileptic seizures represent a sudden and transient change in the synchronised firing of neuronal brain ensembles. While the transition of the collective neuronal activity towards the ictal event is not well understood, some progress has been made using nonlinear time series analysis methods. We present here an analysis of the dynamical regimes of the epileptic activity in three patients suffering from intractable (drug-resistant) seizures, and compare these with the dynamics in rodent epilepsy models. We used the time interval between spikes found in the electroencephalographic recordings as our variable to construct interpeak interval (IPI) time delay plots to study the neuronal interictal (activity between seizures), preictal, and seizure activity. A one-dimensional mapping function was obtained by approximation of the IPI plots with a polynomial. Two main dynamical regimes are obtained from the analysis of the mapping function, derived from the subharmonic bifurcation present in the map: period doubling and intermittency, both of which are observed in human and rat seizures. Hence, our simple model obtained from experimental data captures essential phenomena for the collective dynamics of brain networks, that are found in recordings from human and animal epilepsies. The description of the neuronal dynamics based on one-dimensional maps, widely used in other systems, may prove useful for the understanding of the collective population dynamics of brain activity. © 2003 Elsevier B.V. All rights reserved.

Keywords: Rat seizures; First-return maps; Electroencephalography; Human epilepsy; Period doubling; Intermittency

1. Introduction

Brain function results from the integration, at multiple levels, of the spatio-temporal patterns of cellular activity [15,16]. The mechanisms of generation and maintenance of the several brain rhythms, normal or pathological, can be investigated at different levels of

description, from the molecular to the network level. Mathematical analysis of neuronal activity is revealing that the behaviour of the brain networks cannot be fully described using linear methods, and is providing powerful insights into the collective synchronisation dynamics of the neuronal ensembles. The development of nonlinear time series analysis, based on concepts from nonlinear dynamical systems theory, has fostered the application of these methods for the understanding of the underlying dynamics of complex biological systems [12,59,61]. The framework

* Corresponding author. Tel.: +1-416-813-7715;
fax: +1-416-813-7717.
E-mail address: jlpv@sickkids.ca (J.L. Perez Velazquez).

of deterministic chaos constitutes a novel approach to the analysis of irregular-looking time series, such as voltage recordings from human brains, and offers new avenues to address the question of the global, macroscopic dynamical regimes governing the activity of brain circuits. In general, the framework of nonlinear dynamical systems provides a language adequate to shift between different levels of description and to determine the global collective dynamics of ensembles of connected elements.

Epilepsy is a condition characterised by recurrent periods of variable duration of abnormal synchrony of neuronal firing, termed seizures or ictal events. Between seizures, aberrant behaviour of neuronal networks is manifested in the interictal activity. The interictal spike represents the paroxysmal activation of an “epileptic” neuronal ensemble. Theoretical studies of epilepsy have indicated that there may be a distinctive dynamical regime determining the transition from interictal to ictal events [3,13,24]. Specifically, changes in the state of neuronal firing synchrony (as occurs during transitions between normal brain rhythms or the pathological synchronisation during seizures) can be associated with bifurcations in the system’s dynamics [35]. Bifurcation theory is being used to determine fundamental properties of neuronal activity [25].

Our aim is not so much to provide an accurate theoretical model of neuronal synchrony during seizures, as to elucidate some notable dynamical regimes that take place during the epileptic neuronal activity. We sought to gain insight into the dynamics of epileptiform activity using a geometric approach similar to that used to describe the activity of complex chemical [50], biochemical [10], physical [4] or physiological [7] systems. The knowledge of the specific dynamics, while interesting per se, may also be used for the control of the system’s activity [55,57]. We seek a macroscopic approach that can provide insight into the global dynamical properties of the brain activity leading to the seizure and of the seizure event, by the characterisation of features that are essentially universal. As done in other physical systems [50], we propose a global description of the dynamics of epileptiform activity based on one-dimensional maps. For this purpose, we use the time intervals between

spikes found in the EEG recordings during epileptic activity as our variable to construct interpeak interval (IPI) first-return one-dimensional maps. The analysis of the mapping function reveals that a flip, or subharmonic, bifurcation may occur during the transition to seizure. This type of bifurcation leads to two types of dynamical regimes, type III intermittency or period doubling, that are in fact observed during the recorded epileptiform activity in patients and rodents. While our simple one-dimensional map cannot account for the rich variety of brain dynamics, at least it captures essential phenomena seen during experimental recordings. The results of this study, showing the presence of bifurcation points and metastable states that stabilise transiently, complement current concepts about the spontaneous formation of spatio-temporal patterns of brain activity within the framework of metastability and transient phenomena [15,16,29,30].

2. Methods

2.1. Human electroencephalographic recordings and clinical data

Intracranial EEG recordings were performed in three patients with drug-resistant temporal or parietal lobe epilepsy (the brain area where the epileptic discharges originate), as part of their clinical investigation prior to surgery. Seizure onsets were localised to the hippocampus in two patients with temporal lobe epilepsy, and to the postcentral gyrus in a patient with parietal lobe seizures. The recordings analysed were taken from within the epileptogenic focus. The EEG signals were digitised at 200 Hz (Stellate Systems, Montreal, Canada, and XLTEK, Oakville, Canada).

2.2. Rat intracortical recordings

2.2.1. Electrode implantation and induction of status epilepticus

Chronic bipolar electrodes (Plastics One, Roanoke, VA) were implanted into specific brain areas of male Wistar rats (35–40 days old) using a stereotaxic apparatus. A bipolar stimulating electrode was placed

in the fimbria, stereotaxic coordinates -1.3 mm from Bregma, ML 1.2 mm, DV 4.1 mm, and a recording electrode in the hippocampal CA3 area, -3.8 mm from Bregma, ML 3.3 and DV 4 . After a recovery period of $5-7$ days, animals are placed in an electrically screened Plexyglas chamber. The stimulating electrode is connected to a Grass square pulse stimulator S88K (Grass Instruments, Astro-Med Inc., West Warwick, USA), while the recording electrodes are connected to an AI 402×50 ultra-low noise differential amplifier (Axon Instruments, Union City, CA), a CyberAmp 380 signal conditioner (Axon Instruments), and an analogue–digital converter MP100 (Biopac, Santa Barbara, CA). To produce status epilepticus (continuous presence of seizures), the protocol of Vicedomini and Nadler [60] was used.

2.2.2. Induction of atypical absence seizures

After birth, Long–Evans rat pups were treated with the cholesterol synthesis inhibitor AY9944 (7.5 mg/kg), as described in detail previously [9]. This treatment promotes absence seizures that mimic the human atypical absence epileptic syndrome. Intracortical EEG recordings, starting at P45, are made as detailed above [9]. Electrode placement is confirmed histologically at the end of the experiments by standard histological procedures. All animal manipulations were performed according to the protocols approved by the Hospital for Sick Children Animal Care Committee.

2.3. Analysis methods

Peaks are detected in the EEG traces using a peak-detection algorithm, a graphical-based software written in Visual Basic (Microsoft Corp.) which selects peaks based on amplitude and width criteria (criteria that depend on and are optimised for each data set, Khosravani, Carlen and Perez Velazquez, unpublished observations). Our peak detection inspects for a change in sign between the slopes of successive data points, since normally the spikes in EEG recordings have a sharp rising phase followed by a decay to baseline. Thus, only positive-to-negative are considered as peaks, if the search is implemented “above

baseline”. As many events in these recordings are “below baseline”, we can also search for these and then negative-to-positive slopes are considered as peaks.

First, baseline drift (dc shift) was subtracted using a windowed moving-average filter. After this operation, and given a Gaussian distribution of amplitudes in the signal, the software calculates the mean absolute deviation for the whole trace to be analysed, which is used as the base unit of variation. A multiple of this mean deviation value is then used to select the amplitude threshold for detection. The optimal threshold was estimated visually as well as automatically, performing peak-detection runs with increasing threshold values and construction of a plot of threshold versus number of peaks, from which the optimal value is calculated. Visual inspection of the detected peaks was always performed in several random segments of each trace to ascertain that the estimated threshold revealed the events of interest. The width criteria refers to the time interval between successive peaks, if it is less than a specified value (expressed as frequency) then two peaks are averaged into one, so that false-positive peaks are avoided. Normally, we use a width criteria of 20 Hz, but again that depends on the specific signal and analysis to be performed. For example, if the investigator is interested in selecting bursts of spikes, then a width of 2 Hz, for example, may be desirable, so that the spikes riding on a burst are “fused” into one event.

The software thus calculates the interpeak intervals that are then used to construct a time series of IPIs. First-return scatter plots of the IPI values (measured in seconds) were constructed by plotting one IPI versus the next. A first-return one-dimensional mapping function was obtained by approximating the scatter plot to a nonlinear equation [43]. For curve fitting we use the standard nonlinear least-squares routine, the Levenberg–Marquardt method [47], that minimises a least-squares type of function through iterations. Specifically, the value of the merit function χ^2 , which represents the sum of the squares of the deviations of the theoretical curve from the experimental data points, is minimised. The approximating iterations stop when the χ^2 value reaches a minimum and does not change in successive iterations. The scatter IPI plots were then approximated using this method by

the best fit to an algebraic equation (which we call one-dimensional map). Once obtained, the analysis of the mapping function was performed according to the classical methods in nonlinear dynamics [4,21,23]. The software package INSITE [40] was used to construct the bifurcation diagrams. Maple V software (Waterloo Maple Inc., Waterloo, Canada) was used to solve algebraic and differential equations. Data conversion and specific analysis was performed with the Origin (MICROCAL Software Inc., Northampton, MA) and Acknowledge software package (Biopac, Santa Barbara, CA).

3. Results

3.1. Rationale for using patient and animal data: clinical considerations

We chose three patients suffering from intractable temporal and parietal lobe epilepsy that had interictal spike activity in their intracranial EEG recordings. This is important for us because we use the intervals between peaks (interpeak intervals, IPIs) as the variable that may aid in determining specific dynamical regimes during interictal and ictal (seizure) activity. As mentioned in the introduction, interictal EEG activity represents an abnormal brief synchronisation of the epileptic network, and is present in all epileptic patients to some degree. Our three patients showed abundant interictal activity that allowed us to construct IPI recurrent plots at very different time points during the progression to seizures. In addition, these three patients all presented prominent preictal spike activity, this is the interictal activity preceding the seizure. Preictal activity can be defined as the activity immediately before seizure onset, on the order of seconds or minutes at most, which is not visually identifiable on the EEG as heralding a seizure. In other words, it is not possible for an electroencephalographer to predict an impending seizure by visual on-line analysis of this interictal–preictal EEG (however, nonlinear time series analysis has provided some insight into the usefulness of the preictal period in seizure prediction, see Refs. [13,32,38]). This is

a retrospective labelling of the preictal period, obviously, but definitely a true one, as we know for sure that the ictus occurred. Thus, since our patients had enough preictal EEG spike activity, we were able to assess the differences between the IPI first-return plots during interictal, preictal, and ictal events.

The rat animal model we use in this study is characterised by presenting seizures that mimic human limbic (seizures that spread mostly through hippocampal and cortical brain areas) epilepsy [20,60], and therefore represents an *in vivo* model suitable for experimental manipulations that may shed light on the human condition. The second rat epilepsy model we chose to study mimics atypical absence seizures [9]. While this epileptiform activity is very different from limbic epilepsy (involving the thalamo-cortical circuitry), we sought to explore the possibility that the dynamics of this absence epileptiform activity may be similar, to some extent, to the limbic epilepsies, as suggested in previous studies [54].

3.2. One-dimensional first-return maps of preictal activity: possible route to the seizure

We focused on the recordings obtained from three patients with temporal/parietal lobe epilepsy as well as on recordings from a rat model of temporal lobe seizures as described above. While the neuronal activity could be described by a system of differential equations, a common practice in the study of complex systems is to reduce the multidimensional continuous system to a Poincaré map [4,55]. Following the classical embedding theorems [58,62], Ruelle [51] and Packard et al. [39] proposed that time-delayed phase portraits constructed from a time series of a single variable (voltage for example) have similar properties to the original phase portrait constructed from several independent variables. However, because it is difficult to analyse multidimensional phase portraits, a common practice is to obtain Poincaré sections and, from these, one-dimensional maps [4,50,56]. Specifically, low embedding dimensions have been shown to be able to capture some features of the epileptic EEG data [33], and provided insights into the underlying dynamics of the neuronal activity in other preparations [5].

We used the time interval between peaks in the EEG recordings as the variable to construct an interpeak interval time series, as it was shown that there is no loss of information if amplitude time series data are converted to interval time series, specifically interspike intervals [52,53]. Since we use a peak-detection algorithm that recognises peaks based on amplitudes, this corresponds to a threshold-crossing detector, and the time-delay IPI plot can be considered as a Poincaré section of the original dynamical system [33,52,53]. This geometric approach has been used to study the dynamics of the cardiac system [7,17].

Fig. 1 shows representative intracranial EEG recordings from two patients and the first-return IPI plots obtained during 20–30 s of preictal activity, immediately before the seizure. Notice that, while the IPI first-return plots corresponding to interictal activity long before the seizures did not present any structure regardless of the time window used in their construction (Fig. 6B and C), it is apparent that, during preictal activity just before seizure onset, the points are distributed along an underlying curve. The magnification of two preictal events in Fig. 1A (see also Fig. 6A) reveals the presence of two to three peaks in each burst, hence the short-long IPI sequences that originate the L-shaped plot. This sort of continuous curve produces a one-dimensional map, obtained by a Levenberg–Marquardt fitting of the plot (see Section 2) with an inverted polynomial of the form $IPI_{n+1} = [a + bIPI_n + cIPI_n^2]^{-1}$. This equation provided the best fit to the plots and defines the one-dimensional mapping function, relating successive IPIs [43]. Criteria for assessing the statistical significance of the fit was done as described in Section 2. As observed for other systems, the structure of the preictal first-return plots indicates that it could be governed by a family of underlying deterministic maps. These simple one-dimensional maps may therefore characterise the state of the system by capturing essential phenomena (for example, Kaplan et al. [28] provide another interesting application of these maps to the study of axonal firing dynamics). Interestingly, the IPI plots taken at very short intervals during the ictal events showed concentration of points along the skeleton of the preictal plot (Fig. 6). Thus,

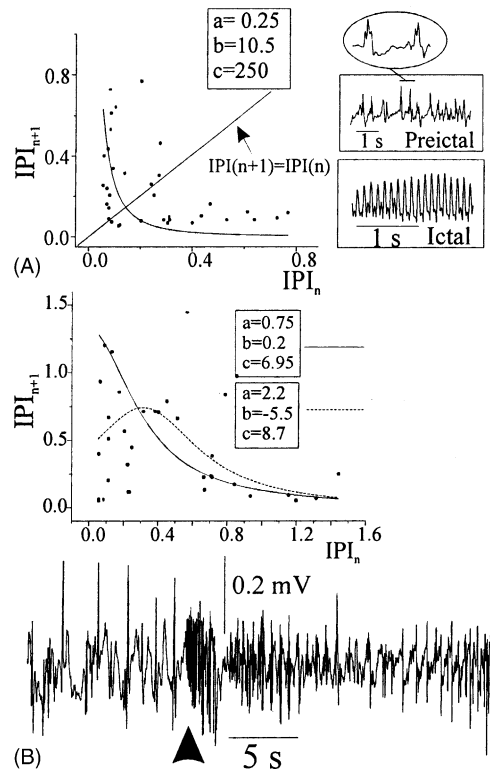


Fig. 1. One-dimensional first-return mapping function for the IPI recursive plot during preictal activity. (A) The scatter IPI first-return plot corresponds to 20 s of preictal activity in a patient with parietal lobe epilepsy, just before the start of the seizure, a segment is shown in the EEG trace on the right (preictal). The “ictal” EEG recording represents the initial ~3 s of the seizure. (B) Another graph obtained from the preictal EEG recording (~30 s) in a patient with left temporal lobe epilepsy. The parameter values in this approximation are shown in the inset. The beginning of the seizure (marked by arrow) is shown in the trace.

apparently, the map is implicitly present in the seizure IPI plots, which will be discussed in detail below in the last section. Now, we would like to concentrate on the mapping function that approximates the preictal scatter plot, and the information we gather from it, as we consider that this is significant to determine the transition to the seizure.

The graph is then approximated by the inverted polynomial with the parameter values shown in the inset in Fig. 1. The inspection of the map reveals the presence of a steady state, the crossing of the map with the diagonal where $IPI_{n+1} = IPI_n$. Steady states here

denote phases of periodic frequencies. The analysis of the specific mapping function mentioned above, with parameter values shown in Fig. 1A, indicates that there is an steady state (solving for $IPI_{n+1} = IPI_n$) at 0.14 s (7.1 Hz) whose slope (dF/dX , with $X = IPI_n$ and F is the mapping function described above) is -1.7 . We are interested in the geometrical characteristics of the fixed points as it has been postulated that this geometry holds the key to understanding the self-organisation of brain dynamics [29,30]. In particular, the slope determines the stability of the equilibrium point, as described in the Hartman–Grobman theorem for maps [22], which states that the stability of the fixed point is determined by the linearisation (dF/dX) of the map at that point. However, when the linearisation, or slope in this case, results in a value of 1 (or -1), the fixed point is termed non-hyperbolic, and, specifically for slopes of -1 , the fixed point is metastable and the map is near a flip (subharmonic) bifurcation [23].

The slope value of -1.7 we obtained, larger than 1 in absolute value, indicates that the fixed point is unstable in this case. The seizure starts (initial 8 s) with a regular activity at 14 Hz, as shown in the ictal EEG recording of Fig. 1A. While the general form of the map function will approximate the preictal activity for the three patients chosen in our study, the specific parameter values a , b and c can change. An exploration of the different steady states for a continuous change in the parameter values is shown in the bifurcation diagram of Fig. 2 and will be detailed in the next section. As another example, Fig. 1B depicts the preictal plot (~ 30 s) leading to a seizure in a second patient with left temporal lobe epilepsy. Two fits are shown, to illustrate the point that several parameter values will yield different approximations to the experimental points. The dotted-line fit is, in this case, a better approximation based on the merit function mentioned in Section 2. The steady state in this case is obtained, as before, by solving for $IPI_{n+1} = IPI_n$ and it results in $IPI = 0.55$ s (1.8 Hz). It is unstable as the slope is -1.2 , close to the metastable value of -1 . The seizure, in this case, starts with a bursting frequency of ~ 1.9 Hz during the initial 7 s after the first burst that was taken as the start of the ictus (EEG trace in Fig. 1B), value close to the frequency ob-

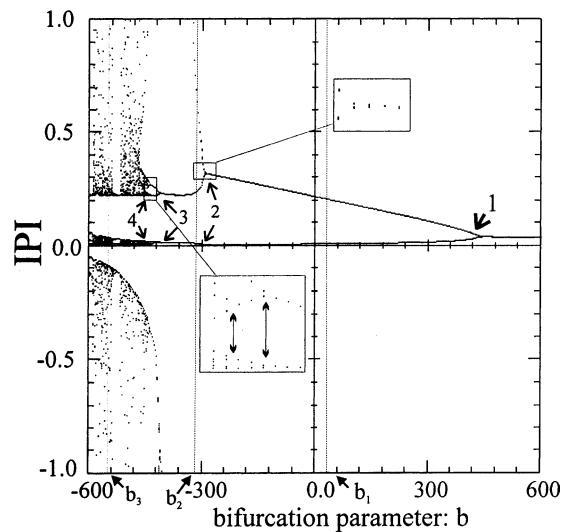


Fig. 2. Bifurcation diagrams for the mapping function. The bifurcation parameter chosen is b (with $a = 4.47$, $c = 2930$, and initial condition $IPI_0 = 0.05$). The IPI values that correspond to equilibrium points are plotted vs. the bifurcation parameter, as explained in the text. To illustrate the points of period doubling (insets), the first four points are labelled with corresponding b values (from right to left) of 468 (1), -280 (2), -410 (3) and -438 (4). Further bifurcation values are not distinguishable. The estimation of the δ value [14], using the third and fourth bifurcation points, yields 4.643, already close to the limiting value of 4.6692. . .

tained from the map at 1.8 Hz, which could represent the transient stabilisation of the unstable steady state, that marks the beginning of the seizure. Visual examination of the general shape of the map (Fig. 1) indicates that there could be a steady state with slope of -1 . Indeed, this will occur for some parameter values. Equilibrium points with slopes of -1 are metastable states, and are termed flip, or subharmonic, bifurcation points as mentioned above [21,23]. Bifurcation points represent a change in the system's dynamics. The determination of possible bifurcations are of great interest as they provide information of specific dynamical regimes that arise from those bifurcation points, and can determine what some investigators have termed phase transitions in brain activity [15,29]. Flip bifurcations give rise to two dynamical regimes, period doubling and type III intermittency [4], depending upon the flip being supercritical or subcritical, respectively (see Ref. [23, pp. 61–63], for a formal mathematical

account). This, in turn, depends on the parameter values. Thus, we should expect that, in some cases, the bifurcation will lead to an intermittent regime with the special characteristics of type III intermittency [4]. In other cases, period doubling (also termed subharmonic cascade) may be found. We show in the next two sections that period doubling arises in our map, and that these two dynamical regimes are found in EEG epileptic recordings.

Thus, the mapping function described above may capture some fundamental collective phenomena present during epileptiform activity. We do not claim that our mapping function is an accurate model of epileptic activity and obviously cannot reveal the rich variety of brain dynamics. However, to further verify that the map provides a relatively good approximation to the dynamics observed, we follow Kantz and Schreiber [27], in that the most severe test to verify the model equation is to iterate and embed the iterates as the original data set. The simulated data should present an “attractor” that resembles the skeleton of the main body obtained from the original data set. Choosing an arbitrary initial condition, and iterating the mapping function, we find that the iterated IPI first-return plots present the shape of those from the experimental EEG recordings, and, depending upon the starting point for the iterations, we can approximate all of the experimental plots (data not shown). Thus, at some level, our first-return map approximates the activity seen in the recordings. We can then use this simple map to provide an interpretation of epileptiform activity based on its geometrical characteristics that determine the transient stabilisation of steady states.

3.3. Bifurcation diagrams of the one-dimensional map

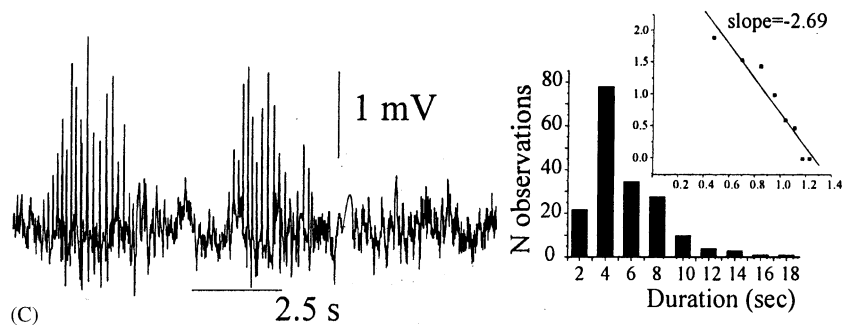
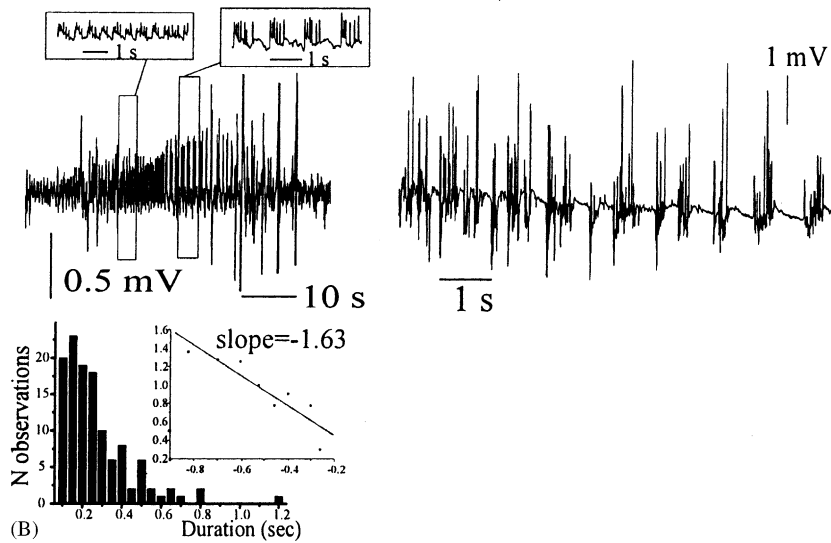
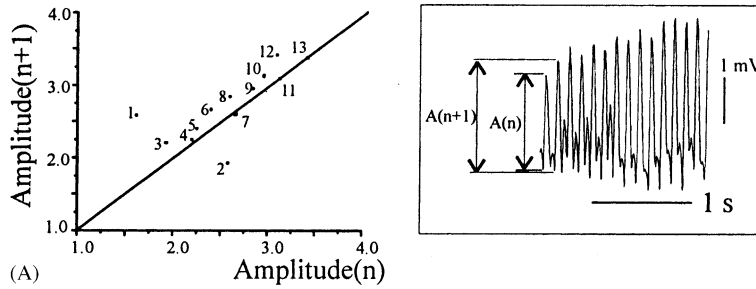
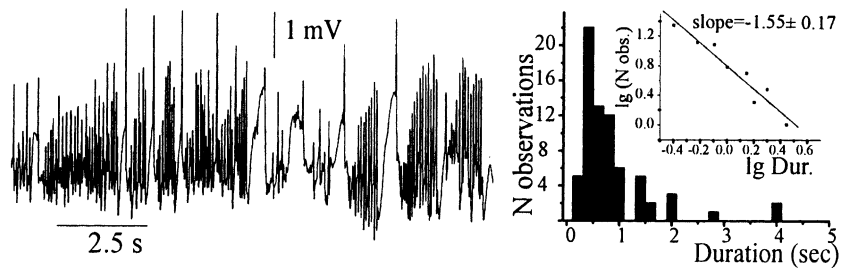
To explore the behaviour of the mapping function for distinct parameter values, we constructed bifurcation diagrams. These graphs indicate the steady state behaviour of a system over a range of parameter values. For these studies, the IPIs are found by successive iterations of the one-dimensional mapping function presented above. Only the IPI values that correspond to equilibrium points are plotted versus the bifurca-

tion parameter value. Fig. 2 shows the bifurcation diagram corresponding to parameter b . A qualitatively similar diagram was obtained for parameters a and c . The important characteristic to note is the period doubling cascade that is evident in the graph: the period doubles at certain parameter values. This diagram has the typical universal scaling property of one-dimensional maps (with an extremum, to be formally precise), in that the δ value [14] approaches the limiting value of 4.6692... These diagrams also reveal the presence of regions where the dynamics could be chaotic, as well as the typical windows of periodicity within that complex region. Regions of periods 2 and 4 are distinguished and labelled in the figure as b_1 and b_2 , respectively, while b_3 is in the complex region.

Thus, the analysis of our simple map uncovers that two specific dynamical regimes may occur during epileptiform activity, period doubling and type III intermittency, arising from a flip, or subharmonic, bifurcation. We will show next that we indeed observe dynamical signatures corresponding to these two regimes in patient and animal EEG recordings during seizures.

3.4. Period doubling and intermittency in EEG recordings during epileptiform activity

Intermittency is probably the clearest dynamical regime seen in all the recordings we obtained. Fig. 3 depicts a few examples in human and animal recordings. Visual inspection already shows the typical signs of the intermittent regime: periods of “laminar”, or almost regular phases [46] interrupted by turbulent (possibly chaotic [4]) periods. Note the similar bursting characteristics between the seizure recording in a patient with right temporal lobe epilepsy (Fig. 3A) and the rat recordings during temporal lobe seizures (Fig. 3B). Shown in Fig. 3C is a recording of a rat during atypical absence seizure activity (described in Section 2 [9]). While being a different type of epileptic syndrome that involves a distinct neuronal circuitry, the periodic bursting activity appearing at irregular intervals is also apparent and common to the previously mentioned limbic seizures.



There are quantitative consequences for the statistics of the laminar phases during intermittency, that differentiates type III versus the other two types. A signature of type III intermittency is revealed by the distribution of the length of the laminar, almost regular, phases [4] as shown in Fig. 3 for all the cases: the concentration of short duration regular periods with a $-3/2$ power-law scaling as seen in the log–log plots (insets in Fig. 3A and B). The regular phases are considered here either the bursts (rhythmic generation of spikes), that have a specific intraburst high-frequency spike activity, or other intervals when the frequency is relatively constant, for example the “ictal” inset in Fig. 1A (also Fig. 3C). Hence, the distribution of the duration of the laminar phases with the concentration at small lengths, as well as the power-law scaling (-1.55 and -1.63) suggest that this intermittency regime is present during seizures in rats and humans. However, while the histogram of the duration of the regular phases is similar in the case of the atypical absence seizures, the power law scaling is different (-2.69 , Fig. 3C). Note that rat atypical absence seizures are distinct from the limbic seizures shown above, and are characterised by the recurrent appearance of 6–7 Hz spike-and-wave activity [9], two of these bursts are shown in the depth thalamic recording in the figure. We would like to note here, however, something that is infrequently mentioned in these kind of studies, regarding the power law distribution of the duration of the laminar phases during intermittency. The typical -1.5 power-law distribution for type III intermittency, in the asymptotic limit, is valid for values of the duration of the regular phases that are neither too short (compared with the fundamental fre-

quency) nor too long. To accurately determine these limits, knowledge of specific control parameters is needed [4], which we do not have when dealing with experimental EEG recordings. Hence, the fact that the distribution corresponding to the regular phases during absence seizures does not satisfy the -1.5 scaling does not necessarily mean it is not type III intermittency, but reflects the limitations of our analysis without a detailed model system (system of differential equations with known control parameters). Further indications of intermittency are found in the first-return amplitude plot shown in Fig. 3A, where the typical walk on the diagonal, characteristic of this dynamical regime, can be appreciated. The value of the amplitude of the large peak, $A(n)$, is plotted versus the next value, $A(n+1)$. The points in the plot have been numbered to illustrate the slow passage along the diagonal. It is worth noting the similarities of this next-amplitude plot with others obtained in completely distinct systems, such as intermittency in chemical reactions (Fig. 2 in [50]).

Period doubling, derived from the bifurcation analysis of the map (Fig. 2), was found in the EEG recordings during seizures in a patient with right temporal lobe epilepsy, as presented in Fig. 4. All seizures in this patient displayed evident period doubling: the length of one period (which technically is defined as a basic pattern that is repeated) “almost” reproduces itself every period and the period length doubles [4,14]. The period is marked by rectangles in the figure. This definition of period doubling is used in some studies, however, there is also another denotation of this phenomenon: the split up of one period into two, such as those in Figs. 2 and 5. The intervals between spikes and associated IPI graphs are not the most adequate

Fig. 3. Signatures of type III intermittency in human and rodent recordings during seizures. (A) EEG recording during the middle of a seizure in a patient with right temporal lobe epilepsy. Notice the transient recurrent appearance of “laminar” phases (bursts) with a very regular, periodic activity. The right-hand side histogram depicts the distribution of the duration of the regular phases and the characteristic power-law distribution seen in the log–log plot in the inset ($r = -0.97$), with a scaling of -1.55 . The graph below is the next-amplitude (or first-return) plot, taken from the measured amplitudes of the EEG peaks during a rhythmic, “laminar” phase in the middle of a seizure in the same patient, shown in the right-hand side recording. See text for details. (B) Seizures in rats with status epilepticus also display characteristics of intermittency. Shown are two depth hippocampal recordings in two different rats. The left recording shows the whole seizure, and the right-hand side trace depicts the activity towards the end of another seizure in another rat. The log–log plot ($r = -0.92$) determines the scaling of the distribution of the duration of the regular phases. (C) Thalamic recordings showing atypical absence seizures in a rat treated with AY-9944, as described in Section 2. The histogram of the distribution of the duration of these “almost regular” bursts shows the concentration in the short duration and the scaling of -2.69 ($r = -0.97$).

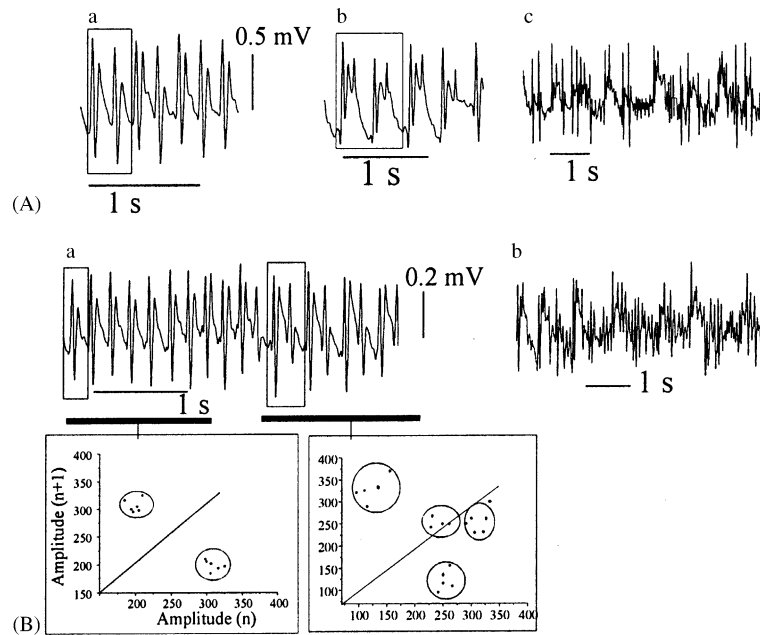


Fig. 4. Period doubling during seizures in a patient with right temporal lobe epilepsy. The intracranial EEG traces show successive recordings. (A) The length of one period is marked by a rectangle. Trace 'c' is during the last seconds of the seizure, note the complex multi-frequency activity. (B) Another seizure in same patient, 'a' and 'b' are successive recordings. Recording in 'b' shows the complex activity at the end of the seizure. The first-return amplitude plots are shown below the corresponding traces.

method to visualise period doubling because the waveforms are not taken into consideration (whatever spike crosses the threshold is considered a peak), and, according to the first definition, it is the waveform that determines the observation of the length of one period. Note, for example, the different peak amplitudes in the recordings of Fig. 4. Visual inspection of the trace 'b' in Fig. 4A reveals that now the activity reproduces itself with a period almost twice (1.97) that of the trace shown in part 'a'. The EEG trace in 'c' shows the continuation of the activity from that of trace 'b', towards the end of the seizure. Note the complex multi-frequency activity. Fig. 4B shows another seizure in same patient, 'a' and 'b' are successive recordings. The length of the second period, marked by the larger rectangle, is 1.98 times the first one (small rectangle). Recording in part 'b' shows the complex activity at the end of the seizure, following the recording shown in 'a'. To consider the waveform shape, the recursive amplitude plot is the standard graph used in other physical systems to study period

doubling [4]. The next-return amplitude plots are shown in Fig. 4B. The resulting scatter plots reveal the presence of two clusters of points for the first part of the trace in 'a', and four clusters for the second half when the period doubles. We could not find period doubling in the EEG samples from the other two patients or in the rat recordings. However, because of the variabilities associated with the recording sites in these kind of experiments, it is significant that an example of this dynamical regime was found and reveals that it is present in, at least, some cases of limbic epilepsy.

Fig. 5 depicts the time evolution of the IPIs during seizures, where we can also appreciate bifurcations. Time is used here as the "bifurcation" parameter. Some evident doubling of the periods (here considering the second interpretation mentioned above, when one period splits up into two) are presented in the insets in Fig. 5A, while small intervals within seizures are shown in Fig. 5B and C, this last is a recording from a rat during status epilepticus activity.

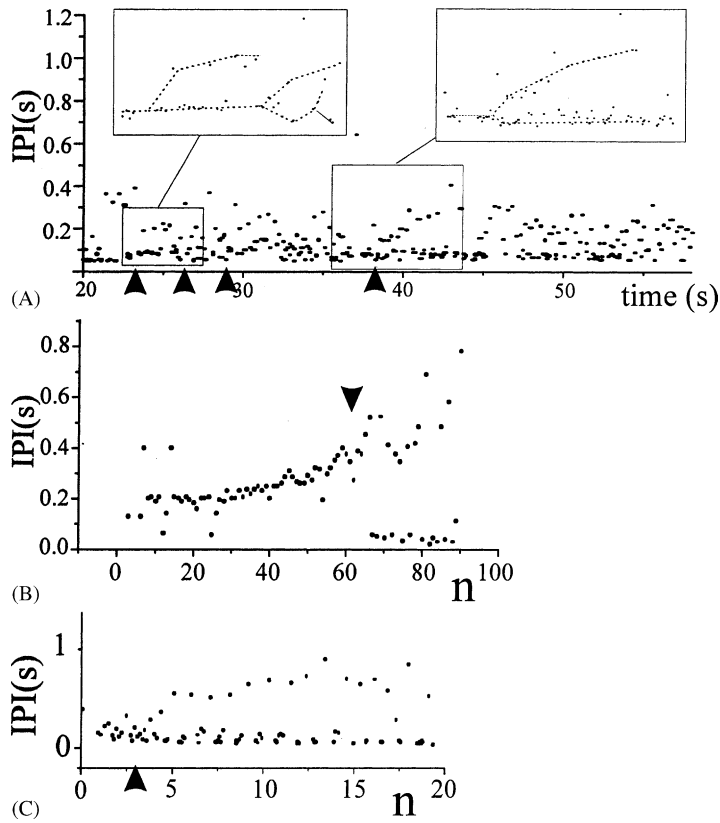


Fig. 5. Bifurcations during seizures. (A) The IPI evolution during most of a 60 s seizure in a patient with right temporal lobe epilepsy. Two of the bifurcations are magnified in the insets. (B) A similar bifurcation that occurred during one seizure in a patient with left temporal lobe epilepsy. The x-axis here is the IPI number (n). (C) Depicts a similar bifurcation structure during a seizure in a rat during a temporal lobe seizure; recording site was the hippocampus.

3.5. A geometric interpretation of epileptiform activity

From our simple mapping function we can obtain a possible interpretation based on its geometrical properties. A qualitative interpretation is presented in Fig. 6. During interictal activity long before the seizure, the IPI plot is space-filling and looks random, as can be seen in the detailed evolution of the recursive IPI plots using short time periods (70 and 24 h before seizures, in Fig. 6B and C) for two different patients. However, the recursive IPI plots for the preictal brain activity preceding the seizure observed in the three patients studied here, presents points distributed along an L-shaped curve that describes the mapping function mentioned above. This is probably

due to the presence of multiple (2–3) peaks in each preictal “burst”, giving rise to the long–short–long intervals, and their more frequent appearance. The critical point to note is the presence of a fixed point that, depending upon the slope, could be stable, unstable, or metastable (if slope is -1 , indicating a flip bifurcation). Thus, iterations of the map, as depicted by arrows in Fig. 6A, will be more or less complex along the underlying curve, sometimes converging on specific areas and determining a periodic oscillation, as seen for example in the preictal recording 20 s (-20 s) preceding the ictus in Fig. 6C (period 2), or during the seizures (SZ2). The transition to the seizure is determined by the (transient) stabilisation of the fixed point, which is achieved geometrically by altering the shape of the map so that the slope at

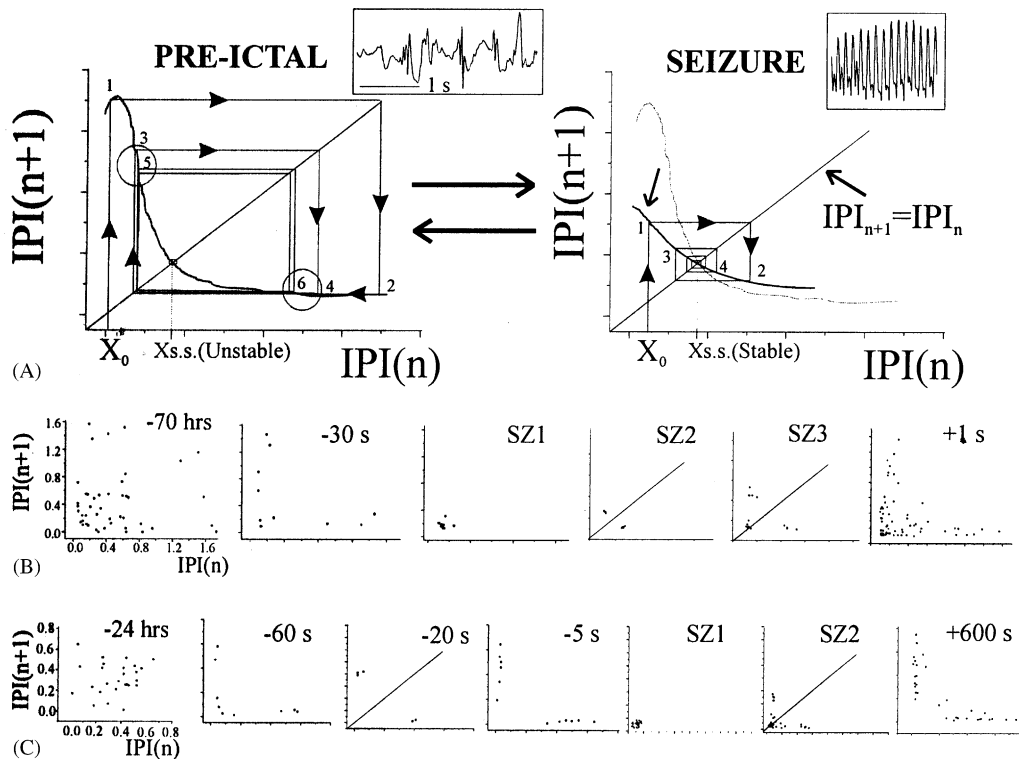


Fig. 6. Geometrical interpretation of epileptiform activity. (A) Hypothetical description based on iterations of the L-shaped map observed during the preictal activity (Fig. 1). The steady state ($X_{s.s.}$) in this case is unstable, therefore the iterates, starting at X_0 and numbered consecutively, converge on a period-2 cycle characterised by long–short intervals, depicted by the circles. If X_0 starts near $X_{s.s.}$, the iterates move away from the fixed point and converge on a similar period-2 cycle (not shown). The inset on top shows a preictal recording from a patient, where the long–short IPIs are apparent. The right-hand side graph shows the now stable steady state, the iterates converging on it, that marks the beginning of the high-frequency seizure firing. (B) IPI recursive plots corresponding to the interictal activity in a patient 70 h before the seizure (–70 h), and short time intervals (~ 6 s each) 30 s (–30 s) before the seizure, during the progression of the seizure (SZ1, SZ2, SZ3), and immediately (1 s) after the seizure. (C) Plots for the transition to the seizure, and during it (SZ1, SZ2), in a different patient taken at short time intervals of ~ 8 s (except for the first one 24 h pre-seizure, because at this time interictal spikes were not as frequent).

the fixed point becomes <1 , shown in the right-hand graph of the figure, labelled “seizure”. The iterations now converge on the stable steady state. This moment corresponds to the appearance of the high-frequency synchronous state that marks the start of the seizure (inset in figure), and can be seen in the IPI plots labelled as SZ1. Changing the shape of the map again may result in the increasing of the slope of the steady state, thus becoming unstable, and the iterations will follow, during this transition, patterns similar to those seen in seizure recordings (Fig. 6B and C). Depending on the shape of the map, clusters of points will materialise in different areas, representing the several frequencies that appear successively during the pro-

gression of the seizures, in what could be considered as the route “out of the seizure”. Examples of this are shown in the IPI plots obtained during seizures from two patients in Fig. 6B and C (SZ1, SZ2, ...). Similar IPI plots are obtained during the ictal events in the case of the rats with status epilepticus (not shown). Note that the postictal IPI plots (+1 and +600 s after the seizure) still show the L-shaped form. Thus, we conclude that the continuous progression of the interictal–preictal–ictal activity, manifested by successive frequencies registered in the EEG, could be captured by the iterations of a one-dimensional map that reveals possible bifurcation points and some dynamical regimes observed in the recordings.

4. Discussion

We have tried to determine possible dynamical regimes and bifurcations that occur during the pathological brain activity in epilepsy. A fundamental property of complex non-equilibrium systems that operate in a metastable dynamic regime is the transient stabilisation of steady states due to instabilities that lead to bifurcations in the dynamics. This concept has been recognised in physiological systems by some investigators [8,15,16,29]. Specifically, brain function has been theorised to manifest as transient dynamical patterns in brain activity [16]. For example, instabilities arising at spectral peaks for alpha and theta brain rhythms evolve towards low-dimensional limit cycles that correspond to seizures, and the crossing of specific stability boundaries mark the distinction between normal state and seizures [49].

Thus, if we consider that “rhythms correspond to a temporal organisation that appears beyond a critical point of instability of a non-equilibrium steady state” [19], we are justified in the study of possible instabilities and bifurcations of neuronal dynamics. Our approach relied on the use of one-dimensional first-return maps, a geometric strategy that has been used to study complex physical and chemical systems [4,50] and has been applied to biology [7,10,18]. The use of low-dimensional maps is justified in the case of highly dissipative systems, like the brain. Geometric approaches are being used in neuroscience [6,25,28–30]. We chose the IPI as the variable to construct the mapping function as it has been useful to unravel dynamical regimes in other neuronal systems [5] and has been applied to epileptic phenomena to describe local regions of interest [33,34]. Theoretical justification in the use of IPIs derives from studies that revealed that amplitude time series can be converted to interspike interval time series with no loss of information [52,53].

The analysis of traces during the epileptiform activity revealed possible bifurcations in the neuronal dynamics during epilepsy. Bifurcations, a central concept in nonlinear dynamical systems theory, are changes in the properties of the dynamics as parameters change. When the system is operating close to a bifurcation,

a very weak stimulus can switch the dynamics. It has been proposed that bifurcations occur during epileptiform activity, specifically that the “epileptic brain” is closer to a bifurcation point than the normal brain [35]. A possible bifurcation parameter in this regard could be the balance between excitatory and inhibitory transmission [36]. Obviously, the dynamics of neurons is dictated by many state variables. However, this approach may serve to identify key parameters that can be used to understand and possibly control that activity. At this global level, the cellular–molecular events that put the system close to a bifurcation may be distinct and varied, but the collective phenomenon is manifested similarly as a hypersynchronous activity in the ensemble, resulting in the ictus.

The bifurcation derived from our map is termed flip, or subharmonic, and leads to two dynamical regimes, period doubling or type III intermittency, both of which are observed in the experimental EEG recordings. Period doubling is a route from periodic activity to complex, aperiodic, possibly chaotic, activity [14]. This dynamical regime was found in all the seizures studied for a patient with right temporal lobe epilepsy. After a few identified period doublings, the activity became very complex, this occurring towards the end of the ictal event. Hence, period doubling cascades during some seizures can lead the neuronal ensemble to a complex activity favouring desynchronisation and therefore leading to the termination of the seizure. Period doubling occurs as parameters change, and we should keep in mind that we are dealing with a system that is continuously evolving where several parameters may be changing rapidly and hence the period doubles fast. We can hypothesise about a few parameters that could be involved in this phenomenon, as these are known to change rapidly during seizures: synaptic inhibitory potentials [41] and direct electrical interactions [11,42]. It would be interesting to assess the role of these cellular mechanisms, in a quantitative manner, as potential control parameters.

The second dynamical regime, type III intermittency, is characterised by the presence of “laminar”, or quasi-regular phases, interrupted by turbulent periods [4,46]. We found signatures of this regime in the human and rat recordings, and was also shown in four

patients in a previous study [43]. The classification of intermittency into types I, II and III is based on the linear instabilities of the periodic trajectories according to Floquet theory [4]. For our purposes, in this study, suffice to say that a characteristic of type III intermittency is that the nonlinearities present in the system tend to destabilise the system's dynamics, favouring the transition from periodic to turbulent activity. Transitions between chaotic and periodic behaviours often occur via intermittency in physical systems [31]. Thus, this dynamical regime can account for the bursting and the presence of periodic, "laminar" phases characteristic of the seizures. Then, the system's nonlinearities support the progressive destabilisation of the bursting and the transition to turbulence, or desynchronised activity that marks the end of the seizure, in an analogous fashion to the above mentioned period doubling cascade. In general, if intermittency is present in brain activity, then type III is probably more adequate for brain function, considering its main characteristic of many short-duration rhythmic episodes. On the other hand, type I is characterised by the opposite: abundance of long-duration regular phases, which would cause the brain activity to fall into long regular periods of activity, something we see physiologically in a few cases, like during slow wave sleep.

A debated issue is whether the experimental recordings represent stationary processes, and, if not, what can we infer from them. It is well known that stationarity of time series is fundamental for some nonlinear time series analysis, such as estimations of correlation dimension. Again, we cannot emphasise enough the fact that the interictal–preictal–seizure activity is continuous, and the transition from one to another state is, many times, extremely subtle and hard to distinguish. The definition of stationarity involves mathematical idealisations almost impossible to establish in finite amounts of experimental data. Some seizures had time intervals of a few seconds that were stationary according to several statistical criteria [63], even though the whole ictal event behaves as non-stationary phenomena [45]. Indications of nonlinear determinism, depending on the recording site, have also been inferred [1,2]. This is again an important consideration, as the recording electrodes are thought to be placed in areas

near or within the epileptic focus, at least those used in these kind of studies. However, that is never genuinely known, and differences in recording sites may be one of the reasons of the variability found in many studies, such as the "chaos in brain" controversy [44,48].

The approach we present in this study could serve to control the activity leading to the seizure. Considering the work of Christini et al. [8], who used a quadratic fit to atrioventricular interval first-return plots (equivalent to our IPIs in EEG recordings) to control cardiac arrhythmias, it is not inconceivable to venture the possible success of a similar method for seizure control. Indeed, some studies have already suggested the usefulness of first-return plots to pace interictal-like activity in vitro using chaos control methods. Our study does not address specifically the problem of the possible chaotic dynamics of epileptiform activity, because, while a clear mathematical concept, chaos is difficult to show in experimental time series [12,48]. However, we note that the preictal IPI plots have a structure that is not space-filling, which is suggestive of chaos as shown qualitatively in the cardiac system using similar first-return maps [17].

Absence and limbic seizures are very different clinical syndromes, however, nonlinear autoregressive analysis has suggested that they may share common dynamics [54]. Our study suggests that intermittency may be a common dynamic characteristic. While the initiating insults that result in seizures are diverse, the collective mechanisms underlying the expression of these events may be similar. It is well known in physics that disparate systems can have similar macroscopic features. Large numbers of constituents gives rise to coherent behaviour, a characteristic of dissipative systems.

In summary, the analysis presented here provides support for the notion of dynamical changes as the neuronal activity progresses, via preictal states, towards the ictal event [26,36–38,43], and supports the idea that dynamical changes occur during the seizure and result in its termination. Beyond the serial computer paradigm, brain research has entered a stage where stable laws are substituted by stochastic processes sensitive to fluctuations. The concept that brain activity possesses metastable dynamics that allows for

rapid changes, without being locked into stable states, endows cognitive functions with great adaptability.

Acknowledgements

Our work was supported in part by grants from the Savoy Foundation and the Hospital for Sick Children Foundation. We would like to thank an anonymous reviewer for suggesting the inclusion of the study shown in Fig. 5, and Drs. A. Lozano and K. Thapar who performed the subdural and depth electrode implantation.

References

- [1] R.G. Andrzejak, K. Lehnertz, F. Mormann, C. Rieke, P. David, C.E. Elger, Indications of nonlinear deterministic and finite-dimensional structures in time series of brain electrical activity: dependence on recording region and brain state, *Phys. Rev. E* 64 (2001) 061907.
- [2] R.G. Andrzejak, G. Widman, K. Lehnertz, C. Rieke, P. David, C.E. Elger, The epileptic process as nonlinear deterministic dynamics in a stochastic environment: an evaluation on mesial temporal lobe epilepsy, *Epilepsy Res.* 44 (2001) 129–140.
- [3] A. Babloyantz, A. Destexhe, Low-dimensional chaos in an instance of epilepsy, *Proc. Natl. Acad. Sci. U.S.A.* 83 (1986) 3513–3517.
- [4] P. Berge, Y. Pomeau, C. Vidal, *Order within Chaos*, Wiley, New York, 1984.
- [5] H.A. Braun, K. Schafer, K. Voigt, R. Peters, F. Bretschneider, X. Pei, F. Moss, Low-dimensional dynamics in sensory biology. 1. Thermally sensitive electroreceptors of the catfish, *J. Comp. Neurosci.* 4 (1997) 335–347.
- [6] C.C. Canavier, J.W. Clark, J.H. Byrne, Routes to chaos in a model of a bursting neuron, *Biophys. J.* 57 (1990) 1245–1251.
- [7] D.J. Christini, J.J. Collins, Control of chaos in excitable physiological systems: a geometric analysis, *Chaos* 7 (1997) 544–549.
- [8] D.J. Christini, K.M. Stein, S.M. Markowitz, S. Mittal, D.J. Slotwiner, M.A. Scheiner, S. Iwai, B.B. Lerman, Nonlinear-dynamical arrhythmia control in human, *Proc. Natl. Acad. Sci. U.S.A.* 98 (2001) 5827–5832.
- [9] M.A. Cortez, C. McKerlie, O. Carter Snead III, A model of atypical absence seizures: EEG, pharmacology, and developmental characterization, *Neurology* 56 (2001) 341–349.
- [10] O. Decroly, A. Goldbeter, From simple to complex oscillatory behaviour: analysis of bursting in a multiply regulated biochemical system, *J. Theor. Biol.* 124 (1987) 219–250.
- [11] F.E. Dudek, R.W. Snow, C.P. Taylor, in: A.V. Delgado Escueta, A.A. Ward, D.M. Woodbury, R.J. Porter (Eds.), *Role of Electrical Interactions in Synchronization of Epileptiform Bursts*, *Advances in Neurology*, vol. 44, Raven Press, New York, 1986, pp. 593–617.
- [12] T. Elbert, W.J. Ray, Z.J. Kowalik, J.E. Skinner, K.E. Graf, N. Birbaumer, Chaos and physiology: deterministic chaos in excitable cell assemblies, *Physiol. Rev.* 74 (1994) 1–47.
- [13] C.E. Elger, K. Lehnertz, Seizure prediction by nonlinear time series analysis of brain electrical activity, *Eur. J. Neurosci.* 10 (1998) 786–789.
- [14] M.J. Feigenbaum, Universal behaviour in nonlinear systems, *Physica D* 7 (1983) 16–39.
- [15] K.J. Friston, Brain function, nonlinear coupling, and neuronal transients, *Neuroscientist* 7 (2001) 406–418.
- [16] K.J. Friston, Transients, metastability and neuronal dynamics, *NeuroImage* 5 (1997) 164–171.
- [17] A. Garfinkel, M.L. Spano, W.L. Ditto, J.N. Weiss, Controlling cardiac chaos, *Science* 257 (1992) 1230–1235.
- [18] L. Glass, M.R. Guevara, A. Shrier, Bifurcation and chaos in a periodically stimulated cardiac oscillator, *Physica D* 7 (1983) 89–101.
- [19] A. Goldbeter, *Biochemical Oscillations and Cellular Rhythms*, Cambridge University Press, Cambridge, 1996.
- [20] J.A. Gorter, E.A. Van Vliet, E. Aronica, F.H. Lopes da Silva, Progression of spontaneous seizures after status epilepticus is associated with mossy fibre sprouting and extensive bilateral loss of hilar parvalbumin and somatostatin-immunoreactive neurons, *Eur. J. Neurosci.* 13 (2001) 657–669.
- [21] J. Guckenheimer, P. Holmes, *Nonlinear Oscillations, Dynamical Systems and Bifurcations of Vector Fields*, Springer, New York, 1983.
- [22] P. Hartman, *Ordinary Differential Equations*, Wiley, New York, 1964.
- [23] F.C. Hoppensteadt, E.M. Izhikevich, *Weakly Connected Neural Networks*, *Applied Mathematical Sciences*, vol. 126, Springer, New York, 1997.
- [24] L.D. Iasemidis, J.C. Sackellares, *Chaos theory and epilepsy*, *Neuroscientist* 2 (1996) 118–126.
- [25] E.M. Izhikevich, Neural excitability, spiking and bursting, *Int. J. Bifurc. Chaos* 10 (2000) 1171–1266.
- [26] H. Jing, M. Takigawa, Comparison of human ictal, interictal and normal non-linear component analyses, *Clin. Neurophysiol.* 111 (2000) 1282–1292.
- [27] H. Kantz, T. Schreiber, *Nonlinear Time Series Analysis*, Cambridge University Press, Cambridge, 1997.
- [28] D.T. Kaplan, J.R. Clay, T. Manning, L. Glass, M.R. Guevara, A. Shrier, Subthreshold dynamics in periodically stimulated squid giant axons, *Phys. Rev. Lett.* 76 (1996) 4074–4077.
- [29] J.A.S. Kelso, *Dynamics Patterns: The Self-Organization of Brain and Behaviour*, MIT Press, Cambridge, 1995.
- [30] J.A.S. Kelso, A. Fuchs, Self-organizing dynamics of the human brain: critical instabilities and Silnikov chaos, *Chaos* 5 (1995) 64–69.
- [31] I.Z. Kiss, J.L. Hudson, Phase synchronization and suppression of chaos through intermittency in forcing of an electrochemical oscillator, *Phys. Rev. E* 64 (2001) 1–8.
- [32] K. Lehnertz, C.E. Elger, Spatio-temporal dynamics of the primary epileptogenic area in temporal lobe epilepsy characterized by neural complexity loss, *Electroencephalogr. Clin. Neurophysiol.* 95 (1995) 108–117.
- [33] M. Le Van Quyen, J. Martinieri, C. Adam, F.J. Varela, Unstable periodic orbits in human epileptic activity, *Phys. Rev. E* 56 (1997) 3401–3410.

- [34] M. Le Van Quyen, C. Adam, J.P. Lachaux, J. Martinieri, M. Baulac, B. Renault, F.J. Varela, Temporal patterns in human epileptic activity are modulated by perceptual discriminations, *Neuroreport* 8 (1997) 1703–1710.
- [35] F.H. Lopes da Silva, J.P.M. Pijn, Epilepsy as a dynamic disease of brain systems, *Adv. Neurol.* 81 (1999) 97–104.
- [36] F.H. Lopes da Silva, J.P.M. Pijn, W.J. Wadmand, Dynamics of local neuronal networks: control parameters and state bifurcations in epileptogenesis, *Prog. Brain Res.* 102 (1994) 359–370.
- [37] F. Mormann, K. Lehnertz, P. David, C.E. Elger, Mean phase coherence as a measure for phase synchronization and its application to the EEG of epilepsy patients, *Physica D* 144 (2000) 358–369.
- [38] V. Navarro, J. Martinierie, M. Le Van Quyen, S. Clemenceau, C. Adam, M. Baulac, F. Varela, Seizure anticipation in human neocortical partial epilepsy, *Brain* 125 (2002) 640–655.
- [39] N.H. Packard, J.P. Crutchfield, J.D. Farmer, R.S. Shaw, Geometry from time series, *Phys. Rev. Lett.* 45 (1980) 712–716.
- [40] T.S. Parker, L.O. Chua, *Practical Numerical Algorithms for Chaotic Systems*, Springer, Berlin, 1989.
- [41] J.L. Perez Velazquez, P.L. Carlen, Synchronization of GABAergic interneuronal networks in seizure-like activity in the rat entorhinal–hippocampal slice, *Eur. J. Neurosci.* 11 (1999) 4110–4118.
- [42] J.L. Perez Velazquez, P.L. Carlen, Gap junctions, synchrony and seizures, *Trends Neurosci.* 23 (2000) 68–74.
- [43] J.L. Perez Velazquez, H. Khosravani, A. Lozano, B.L. Bardakjian, P.L. Carlen, R. Wennberg, Type III intermittency in human partial epilepsy, *Eur. J. Neurosci.* 11 (1999) 2571–2576.
- [44] J.P. Pijn, J. van Neerven, A. Noest, F.H. Lopes da Silva, Chaos or noise in EEG signals: dependence on state and brain site, *Electroencephalogr. Clin. Neurophysiol.* 79 (1991) 371–381.
- [45] J.P. Pijn, D.N. Velis, M.J. van der Heyden, J. DeGoede, C.W. van Veerlen, F.H. Lopes da Silva, Nonlinear dynamics of epileptic seizures on basis of intracranial EEG recordings, *Brain Topogr.* 9 (1997) 249–270.
- [46] Y. Pomeau, P. Manneville, Intermittent transition to turbulence in dissipative dynamical systems, *Commun. Math. Phys.* 74 (1980) 189.
- [47] W.H. Press, S.A. Teukolsky, W.T. Vetterling, B.P. Flannery, *Numerical Recipes in C. The Art of Scientific Computing*, Cambridge University Press, Cambridge, 1999.
- [48] P.E. Rapp, A guide to dynamical analysis, *Integr. Physiol. Behav. Sci.* 29 (1994) 3111–3127.
- [49] P.A. Robinson, C.J. Rennie, D.L. Rowe, Dynamics of large-scale brain activity in normal arousal states and epileptic seizures, *Phys. Rev. E* 65 (2002) 041924.
- [50] J.-C. Roux, Experimental studies of bifurcations leading to chaos in the Belousof–Zhabotinsky reaction, *Physica D* 7 (1983) 57–68.
- [51] D. Ruelle, Sensitive dependence on initial conditions and turbulent behaviour of dynamical systems, *Ann. N.Y. Acad. Sci.* 316 (1979) 408.
- [52] T. Sauer, Reconstruction of dynamical systems from interspike intervals, *Phys. Rev. Lett.* 72 (1994) 3811–3814.
- [53] T. Sauer, Interspike interval embedding of chaotic signals, *Chaos* 5 (1995) 127–132.
- [54] N.D. Schiff, D.R. Labar, J.D. Victor, Common dynamics in temporal lobe seizures and absence seizures, *Neuroscience* 91 (1999) 417–428.
- [55] T. Shinbrot, C. Grebogi, E. Ott, J.A. Yorke, Using small perturbations to control chaos, *Nature* 363 (1993) 410–417.
- [56] H.L. Swinney, Observations of order and chaos in nonlinear systems, *Physica D* 7 (1983) 3–15.
- [57] T. Takahiro, N. Inaba, J. Miyamichi, Mechanisms for taming chaos by weak harmonic perturbations, *Phys. Rev. Lett.* 83 (1999) 3824–3827.
- [58] F. Takens, *Detecting Strange Attractors in Turbulence*, Lecture Notes in Mathematics 898, Springer, New York, 1981.
- [59] M.S. Titcombe, L. Glass, D. Guehl, A. Beuter, Dynamics of Parkinsonian tremor during deep brain stimulation, *Chaos* 11 (2001) 766–773.
- [60] J.P. Vicedomini, J.V. Nadler, A model of status epilepticus based on electrical stimulation of hippocampal afferent pathways, *Exp. Neurol.* 96 (1987) 681–691.
- [61] B.J. West, *Fractal Physiology and Chaos in Medicine*, World Scientific, Singapore, 1990.
- [62] H. Whitney, Differentiable manifolds, *Ann. Math.* 37 (1936) 645.
- [63] S.M. Zoldi, A. Krystal, H.S. Greenside, Stationarity and redundancy of multichannel EEG data recorded during generalized tonic–clonic seizures, *Brain Topogr.* 12 (2000) 187–200.